



Published in final edited form as:

J Med Chem. 2008 August 28; 51(16): 4968–4977. doi:10.1021/jm800512z.

Structure Based Development of Phenyl-imidazole-derived Inhibitors of Indoleamine 2,3-Dioxygenase

Sanjeev Kumar¹, Daniel Jaller², Bhumika Patel¹, Judith M. LaLonde^{1,*}, James B. DuHadaway², William P. Malachowski^{1,*}, George C. Prendergast^{2,3}, and Alexander J. Muller^{2,*}

¹Department of Chemistry, Bryn Mawr College, Bryn Mawr, Pennsylvania 19010, USA

²Lankenau Institute for Medical Research, Wynnewood, Pennsylvania 19096, USA

³Department of Pathology, Anatomy & Cell Biology and Kimmel Cancer Center, Thomas Jefferson University, Philadelphia, Pennsylvania 19104, USA

Abstract

Indoleamine 2,3-dioxygenase (IDO) is emerging as an important new therapeutic target for the treatment of cancer, chronic viral infections, and other diseases characterized by pathological immune suppression. With the goal of developing more potent IDO inhibitors, a systematic study of 4-phenyl-imidazole (4-PI) derivatives was undertaken. Computational docking experiments guided design and synthesis efforts with analogs of 4-PI. In particular, three interactions of 4-PI analogs with IDO were studied: the active site entrance, the interior of the active site and the heme iron binding. The three most potent inhibitors (**1**, **17** and **18**) appear to exploit interactions with C129 and S167 in the interior of the active site. All three inhibitors are approximately ten-fold more potent than 4-PI. The study represents the first example of enzyme inhibitor development with the recently reported crystal structure of IDO and offers important lessons in the search for more potent inhibitors.

Introduction

Immune escape by tumors is a fundamental aspect of disease progression resulting from immunoediting of tumors as they interact with the host immune system¹. Key to this process from a therapeutic standpoint is that tumors are selected to actively suppress the ability of the immune system to mount an effective response through the establishment of a tolerogenic microenvironment that dominantly suppresses treatment strategies aimed at eliciting antitumor immune activation². Ongoing progress in understanding the cellular and molecular mechanisms that shape the pathological state of tumoral immune tolerance has revealed a complex web of interactions between both tumor cells and stromal cells in which a number of potential therapeutic targets for intervention with small molecule inhibitors have been identified³. One central player is the immunomodulatory enzyme indoleamine 2,3-dioxygenase (IDO). IDO can contribute to immune escape when expressed directly in

*Address correspondence regarding the chemistry to William P. Malachowski at the Department of Chemistry, Bryn Mawr College, 101 N. Merion Ave., Bryn Mawr, PA 19010-2899; phone: 610-526-5016; fax: 610-526-5086; wmalacho@brynmawr.edu.. *Address correspondence regarding the computational experiments to Judith M. LaLonde at the Department of Chemistry, Bryn Mawr College, 101 N. Merion Ave., Bryn Mawr, PA 19010-2899; phone: 610-526-5679; fax: 610-526-5086; jlalonde@brynmawr.edu.. *Address correspondence regarding the biology to Alexander J. Muller or George C. Prendergast at Lankenau Institute for Medical Research, Wynnewood, PA 19010; phone: 610-645-8034; fax: 610-645-2095; mullera@mlhs.org..

SUPPORTING INFORMATION PARAGRAPH Copies of ¹H and ¹³C NMR spectra and liquid chromatograms for compounds **1–5**, **8–11**, **13–18**, **23**, **24**, and **30**. Copies of liquid chromatograms for **6,7,12**, and **29**. Table of CHelpG charges for compounds **1,2**, **4–6**, **8**, **9**, **17** and **18**. Eadie-Hofstee plots for **17** and **18**. This material is available free of charge via the Internet at <http://pubs.acs.org>.

tumor cells or when expressed in immunosuppressive antigen presenting cells such as tolerogenic dendritic cells or tumor associated macrophages.^{4, 5} Either way, experimental results suggest that IDO inhibition may restore the capacity to stimulate an effective antitumor immune response and thus provide a method to treat malignant diseases in combination with chemotherapeutic agents and/or immunotherapy-based strategies⁶.

IDO is an extrahepatic, tryptophan (Trp) metabolizing enzyme,⁷⁻⁹ which catalyzes the initial and rate-limiting step along the kynurenine pathway. The oxidative metabolism of Trp by IDO involves the addition of oxygen across the C-2/C-3 bond of the indole ring. IDO coordinates molecular oxygen to a heme iron in the ferrous oxidation state. Only the ferrous oxidation state is catalytically active. Oxidation of the heme iron to the ferric state creates an inactive form of the enzyme which requires reduction prior to Trp and oxygen binding.

The most frequently used inhibitor of IDO, 1-methyl-tryptophan (1-MT), has a reported K_i of 34 μM ^{10, 11}; only recently have nanomolar level inhibitors been reported in the scientific literature.¹²⁻¹⁵ In 1989, 4-phenyl-imidazole (4-PI) was identified as a weak noncompetitive inhibitor of IDO¹⁶. Despite the noncompetitive inhibition kinetics, Sono and Cady demonstrated through impressive spectroscopic studies that 4-PI was binding to the heme iron at the active site. Furthermore, a preference for binding to the ferric versus the ferrous form of the enzyme was discovered. Presumably, the noncompetitive inhibition kinetics was the result of preferential binding for the inactive ferric form of IDO.

More recently, the first crystal structure of IDO was reported¹⁷ and it confirmed the results of Sono and Cady by showing 4-PI bound to the heme iron (Fig. 1). With the rich structural information found in the crystal structure, we began a structure-activity study of 4-PI analogs to probe the active site and discover more potent IDO inhibitors. Our structural modifications to the 4-PI skeleton were focused on exploiting three binding interactions with IDO: (1) the active site entrance region defined by the heme 7-propionic acid group and occupied by the N-cyclohexyl-2-aminoethanesulfonic acid (CHES) buffer molecule in the crystal structure; (2) the interior of the active site, in particular interactions with C129 and S167; (3) the heme iron binding group. We hoped to achieve interactions with the active site entrance region through substitution on the imidazole ring. The interior region of the active site would be probed through substitution on the phenyl ring of 4-PI. The heme iron binding interaction would be explored by replacement of the imidazole ring with other heterocycles or, more subtly, through electronic changes caused by phenyl group substitution. The results of our study are described herein and include a ten-fold improvement in 4-PI potency. Two of the most potent inhibitors in the study illustrate the benefits of using sulfur moieties over oxygen or fluorine to enhance protein-ligand interactions in the binding site of IDO.

Chemistry

The 4-phenyl-imidazole derivatives were synthesized using precedented protocols or procedures adapted from the literature. De novo imidazole ring synthesis occurred through the reaction of α -bromo-ketones with formamide (Scheme 1).¹⁸ The 2,6-dimethoxy-acetophenone precursor of **10** was also synthesized by reaction with formamide and the methyl ethers were cleaved with HBr to generate **11**. The nitrile group of **6** was reduced to an aldehyde (**12**, not shown) by literature protocols.¹⁹

Thioether substituted phenyl derivatives (**13-15**) were synthesized through Suzuki coupling reactions (Scheme 2). Demethylation was accomplished under alkali metal reduction conditions to provide the thiophenols (**16-18**).^{20, 21}

N-1 Alkylated derivatives of the 4-phenyl-imidazoles were synthesized by deprotonation with sodium hydride and alkylation (Scheme 3). The N-1 aminoalkyl substituents were

masked as phthalimide groups and subsequently deprotected with hydrazinolysis to afford **23** and **24**.

Alkylation of the N-3 imidazole position was accomplished by first protecting the N-1 position with acrylonitrile (**25**, Scheme 4).²³ Benzylation of the N-3 position generated quaternary salt **26** which was deprotected with NaOH to afford **27**.

C-2 Imidazole derivatives were synthesized by N-1 trityl protection, followed by lithiation and formylation (Scheme 5). The aldehyde **28**²⁴ was reduced to the alcohol **29**²⁴ or converted to the methylamine **30** by reductive amination. All other 4-phenyl-imidazole derivatives were synthesized according to literature procedures or were commercially available.

Results

IDO inhibition through interactions at the active site entrance

The N-1, C-2, and N-3 positions of the imidazole ring were substituted with the goal of appending groups that would occupy the active site entrance. In the crystal structure of 4-PI with IDO, this region contains a CHES buffer molecule whose alkyl portion forms hydrophobic interactions with F163 and F226. In addition, the amino group of the CHES molecule forms an ion pair with the heme 7-propionic acid. However, our attempts to form an ionic or hydrogen bond with the heme 7-propionic acid group, or a hydrogen bond to other residues in the entrance to the binding site (i.e. S263 or R231) all failed (Table 1, **23**, **24**, **29** and **30**).

The absence of activity with N-1 substituted 4-PI derivatives **19** and **20** confirms the binding of the N-1 nitrogen to the heme iron and demonstrates that the N-3 nitrogen of the imidazole can not substitute to bind at the heme iron. Moreover, our docking experiments showed N-3 substitution should be permitted and indeed the N-3 benzyl substituted derivative **27** was roughly equipotent to 4-PI; thereby demonstrating that imidazole ring substitution is tolerable. Compound **27** also fits the pharmacophore that was developed in studies of IDO inhibition by brassinin derivatives, i.e. a heme iron binding group flanked by two aromatic structures.²⁵

IDO inhibition through interactions in the interior of the active site

Analysis of the crystal structure of 4-PI bound to IDO¹⁷ indicated that S167 and C129 were in close proximity to the phenyl ring. We proposed systematic ortho, meta and para substitutions of the phenyl ring with oxygen, sulfur and fluorine to ascertain if specific protein-ligand interactions could be exploited. Docking experiments conducted with Gold (version 3.1)^{27, 28} predicted hydrogen bonds between the 2- or 3-hydroxy and S167 (Figure 2). Furthermore, docking was suggestive of a disulfide bond or a weak hydrogen bond²⁹⁻³⁵ between the 3- or 4-thiol substituted phenyl and C129. The fluoro-substituted analogs were synthesized to serve as a bioisostere to the OH substitutions or to enhance potency through other potential polar interactions with the protein.³⁶

The 2-hydroxy modification (**1**) afforded the most success (Table 2) generating a ten-fold increase in potency relative to 4-PI. Presumably, the 2-hydroxy group is forming a hydrogen bond with the S167, although the crystal structure indicates the 2-hydroxy group can rotate away from S167 by spinning about the phenyl-imidazole bond. The 2,6-dihydroxy-phenyl derivative **11**, which presents a hydroxy group to S167 in either rotamer, supports the presence and significance of the hydrogen bond to S167 since it is roughly equipotent to **1**.

The 2-thiomethoxy **13** and 2-thiol **16** both lead to modest increases in potency relative to 4-PI, while the 2-fluoro **2** reduced binding affinity. Docking experiments indicated that both sulfur ortho substituents were tolerated and that a hydrophobic contact may form with Y126 for **13**. Alternatively for **16**, docking studies indicated that the thiol group might form an SH- π interaction with F163. Finally, the thiol of **16** is also positioned correctly to serve as a hydrogen bond donor to S167. The weaker potency of the thiol group of **16** versus the hydroxy group of **1** and the dihydroxy derivative **11** is consistent with the greater hydrogen bond enthalpies of OH—O versus OH—S.³²

Modifications in the meta position focused on interacting with C129 located along the roof of the IDO active site (Figure 1). The most potent example in this regard was the meta thiol derivative **17**, which demonstrated a six-fold increase in potency versus 4-PI. Although disulfide formation between the thiol and the C129 side chain was considered possible, no evidence for irreversible inhibition was seen in the enzyme assays. Nonetheless, a weak hydrogen bond (~ 1 kcal/mol)³² with C129 could also explain the six-fold increase in potency. Alternatively, docking indicated that the 3-thiol-phenyl ring may rotate, so that the 3-thiol serves as a H-bond acceptor to S167. In the absence of structural information which could confirm predicted binding modes, either interaction may account for the increased affinity for this substitution. Hydroxy and fluoro hydrogen bonding donors and acceptors in the meta position failed to enhance the activity of the 4-PI structure. While docking indicates that either substitution could bind with favorable interactions to either S167 or C169, the optimal distance for a hydrogen bond interaction with either residue may be achieved with the larger thiol group.

Nitrile **7** and aldehyde **12** were synthesized to exploit the well-known nucleophilicity of thiol groups,^{37–39} such as that found in C129. However, based on the absence of irreversible inhibition kinetics with these compounds, neither the nitrile nor the aldehyde engaged in any reaction with the thiol of C129.

Thiol substitution in the para position (**18**) also generated a six-fold increase in IDO inhibitor potency. Similar to **17**, enzyme inhibition assays did not support irreversible binding through disulfide bond formation. No other modification in the para position increased potency relative to 4-PI. Examination of the surface complementarity between the docked model of **18** in IDO suggests that it may bind in a small hydrophobic crevice between C129, F164 and L234. Most interestingly, the SAR of ortho, meta and para-SH substitution indicates that thiol clearly enhances protein ligand interactions over F and OH at the meta and para positions. In the absence of structural information, our working hypothesis is that a stronger thermodynamic interaction exists between the thiol of C129 and the sulfur of **18** versus oxygen (**8**) or fluorine (**9**).³²

IDO inhibition through modifications to heme iron binding: alternative aromatic rings

To probe the effect of heterocycle binding to the heme iron, we substituted other aromatic rings for the imidazole of 4-PI. These changes almost universally led to less potent compounds relative to 4-PI (Table 3). For instance, pyridine (**7**, **33** or **36**), thiazole (**34**), pyrazole (**35**), and furan (**36**) all failed to demonstrate any inhibition. Presumably the thiazole, pyrazole and furan fail to bind to the heme iron with the same affinity as the imidazole, a well-known iron ligand in nature, e.g. histidine. Nevertheless pyridine is generally considered to be a better ligand of ferrous heme iron^{40, 41}, the active form of IDO, than imidazole, which is considered a stronger ligand for ferric heme iron¹⁶. However, none of the compounds containing pyridine demonstrated activity better than 4-PI. The poor results with pyridine derivatives might be due to steric factors that limit IDO's ability to accommodate the larger six member ring directly over the heme iron. The replacement of the phenyl group of 4-PI with thiophene was permitted, although there was approximately a

five-fold loss in activity. Only when hydroxy groups were returned to the phenyl ring of pyrazole compounds **31** and **32** was the activity restored or modestly improved over 4-PI. It is likely that these hydroxy groups are exploiting the same hydrogen bonding interactions with the S167 as seen with **1** and **11**. Nevertheless, these studies demonstrate that the imidazole group is optimal both in terms of iron binding strength and shape complementarity.

IDO inhibition through modifications to heme iron binding: a quantum mechanical study of substituent effects on the electrostatic potential of the imidazole ring

As reported by Gaspari et al,²⁵ the binding affinity of the dithiocarbamate IDO inhibitors correlated with the electrostatic potential of the moiety purported to coordinate the heme iron. In the dithiocarbamate study, as the charge on the coordinating atom decreased, there was an increase in binding affinity to the heme iron based on a lower inhibition constant with IDO. The previously described ortho, meta, or para substitutions of the phenyl ring in 4-PI (Table 2) can affect the charge distribution on the imidazole ring of 4-PI through inductive effects and thereby modulate the binding affinity to the heme iron. To probe these electronic effects to the imidazole ring, the quantum mechanical geometry optimizations were calculated and the electrostatic potential was mapped onto the electron distributions for nine phenyl compounds derivatized with hydroxyl (**1**, **4**, **8**), thiol (**16**, **17**, **18**) or fluoro (**2**, **5**, **9**) groups. These calculations determined that there was no appreciable difference in the electronic charge on the iron coordinating imidazole nitrogen due to these substitutions (Supporting Information). Consequently, we conclude that the increase in binding affinity for the designed thiol (**17** and **18**) and hydroxyl (**1**) phenyl-imidazole analogs results from specific protein-ligand interactions rather than ligand electronic effects.

More detailed kinetic analysis was performed on the most potent 4-PI derivatives, **1**, **17** and **18**. Inhibition constants for **1**, **17** and **18** (Table 4) were found to closely resemble the IC₅₀ values. Interestingly, all three showed the best graphical match to an uncompetitive inhibition mode (Figure 3 and Supporting Information), although non-competitive or mixed inhibition modes also demonstrated a good fit. The original report¹⁶ of 4-PI inhibition described noncompetitive inhibition with D-Trp, nevertheless a switch between a noncompetitive and uncompetitive mode of inhibition in IDO is not without precedent. In fact, a similar observation was made with β -carboline.^{16, 45} This apparent switch between non- and uncompetitive inhibition modes, probably indicates an extremely close affinity for two different forms of the IDO enzyme. For example, these inhibitors may have similar affinity for the ferric and ferrous forms of the enzyme and subtle differences in the assay conditions may lead to an apparent switch in the inhibition mode.

Conclusion

Utilizing the recently reported enzyme crystal structure,¹⁷ more potent IDO inhibitors have been designed and developed. Importantly, the best inhibitors (**1**, **17** and **18**) are roughly ten-fold more potent than 4-PI and appear to successfully exploit interactions with two residues in the IDO active site, S167 and C129. Two of these compounds demonstrated the benefits of thiols over hydroxy groups in enhancing protein-ligand interactions. Less potent 4-PI derivatives demonstrate the limitations to modifications of the 4-PI structure. Future work will seek to further exploit the successes communicated herein with the goal of generating even more potent IDO inhibitors.

Experimental Section

Chemistry

General Procedures—All reactants and reagents were commercially available and were used without further purification unless otherwise indicated. Anhydrous CH_2Cl_2 was obtained by distillation from calcium hydride under nitrogen. Anhydrous MeOH was obtained by distillation from Mg metal under nitrogen. Anhydrous THF was freshly distilled from Na and benzophenone. All reactions were carried out under an inert atmosphere of argon or nitrogen unless otherwise indicated. Concentrated refers to the removal of solvent with a rotary evaporator at normal water aspirator pressure followed by further evacuation with a two-stage mechanical pump. Thin layer chromatography was performed using silica gel 60 Å pre-coated glass or aluminum backed plates (0.25 mm thickness) with fluorescent indicator, which were cut. Developed TLC plates were visualized with UV light (254 nm), iodine or KMnO_4 . Flash column chromatography was conducted with the indicated solvent system using normal phase silica gel 60 Å, 230–400 mesh. Yields refer to chromatographically and spectroscopically pure (>95%) compounds, except as otherwise indicated. All new compounds were determined to be >95% pure by NMR, HPLC and/or GC as indicated. Melting points were determined using an open capillary and are uncorrected. ^1H and ^{13}C NMR spectra were recorded at 300 and 75 MHz, respectively. Chemical shifts are reported in δ values (ppm) relative to an internal reference (0.05% v/v) of tetramethylsilane (TMS) for ^1H NMR and the solvent peak in ^{13}C NMR. Peak splitting patterns in the ^1H NMR are reported as follows: s, singlet; d, doublet; t, triplet; q, quartet; m, multiplet; br, broad. ^{13}C experiments with the attached proton test (APT) sequence have multiplicities reported as δ_u (up) for methyl and methine, and δ_d (down) for methylene and quaternary carbons. Normal phase HPLC (NP-HPLC) analysis was performed with UV detection at 254 nm and a 5 μ silica gel column (250 \times 4.6 mm) eluted with a mixture of *n*-hexane and 2-propanol at 0.5 or 1 mL/min. Reverse phase HPLC (RP-HPLC) analysis was performed with UV detection at 254 nm and a 4 μ SYNERGI Hydro-RP 80A® (250 \times 4.6 mm). IR data was obtained with an FT-IR spectrometer. MS data was recorded with atmospheric pressure chemical ionization (APCI) or atmospheric pressure electrospray ionization (APESI) mode.

General procedure for imidazole synthesis—A solution of bromoacetyl derivative (1 mmol) was heated (170–180 °C) in formamide (15 mL) for 5–9 h. After cooling to rt, the reaction mixture was diluted with satd. NaHCO_3 (20 mL) and the aqueous layer was extracted with EtOAc (3 \times 50 mL). The combined organic extract was dried (Na_2SO_4) and concentrated *in vacuo* to afford the crude product which was purified by column chromatography to yield the final product.

2-(1H-imidazol-4-yl)phenol (1)—Synthesized from 2-(2-bromoacetyl)phenol⁴⁶ and formamide according to the general procedure to afford **1** as brown solid in 49% yield. mp=174–175 °C (lit.⁴⁷ mp 174–175 °C. TLC R_f =0.32 (20% MeOH: CHCl_3). ^1H NMR ($\text{CDCl}_3 + \text{CD}_3\text{OD}$) δ 7.64 (s, 1H), 7.49 (d, 1H, J =7.71 Hz), 7.34 (s, 1H), 7.11 (t, 1H, J =7.20 Hz), 6.93 (d, 1H, J =8.13 Hz), 6.84 (t, 1H, J =7.47). ^{13}C NMR ($\text{CDCl}_3 + \text{CD}_3\text{OD}$) δ_d 156.3, 139.3, 119.3; δ_u 135.2, 128.9, 126.7, 120.6, 117.5, 115.4. IR (KBr) 3207, 2602, 1583 1488 cm^{-1} . NP-HPLC t_R =8.41 (40:60, 2-propanol:*n*-hexane, 1mL/min). MS m/z 160.

4-(2-Fluorophenyl)-1H-imidazole (2)—Synthesized from 2-bromo-(2-fluorophenyl)ethanone⁴⁸ and formamide according to the general procedure to afford **2** as an off-white solid in 52% yield. mp=107–108 °C. TLC R_f =0.25 (10% MeOH: CHCl_3). ^1H NMR (CDCl_3) δ 11.2 (br s, 1H), 8.00–7.95 (m, 1H), 7.73 (s, 1H), 7.53 (d, 1H, J =3.09 Hz), 7.24–7.07 (m, 3H). ^{13}C NMR (CDCl_3) δ_d 159.3 ($J^1_{\text{C-F}}$ =246.32 Hz), 132.8, 121.1 ($J^2_{\text{C-F}}$ =12.77

Hz); δ_u 135.6, 128.0 (J^3_{C-F} =8.31 Hz), 127.51 (J^3_{C-F} =3.83 Hz), 124.5 (J^4_{C-F} =3.15 Hz), 119.0 (J^3_{C-F} =11.49 Hz), 115.98 (J^2_{C-F} =21.97 Hz). IR (KBr) 3080, 3005, 2839, 1678 cm^{-1} . NP-HPLC t_R =5.29 (30:70, 2-propanol:n-hexane, 1 mL/min) mixture of two isomers. GC m/z 162.

4-(thiophen-2-yl)-1H-imidazole (3)—Synthesized from 2-bromo-1-(thiophen-2-yl)ethanone⁴⁹ and formamide according to the general procedure to afford **3** as brown crystalline solid in 60% yield. mp=126–127 °C. TLC R_f =0.62 (20% MeOH:CHCl₃). ¹H NMR (CDCl₃) δ 7.60 (s, 1H), 7.23–7.20 (m, 2H), 7.15 (d, 1H, J =4.98 Hz), 6.98 (dd, 1H, J =3.75, 1.05 Hz). ¹³C NMR (CDCl₃) δ_d 136.7, 134.4; δ_u 135.6, 127.8, 123.6, 122.5, 114.2. IR (KBr) 3115, 3080, 2872, 1658 cm^{-1} . NP-HPLC t_R =5.85 (30:70, 2-propanol:n-hexane, 1 mL/min). MS m/z 150.

3-(1H-imidazol-4-yl)phenol (4)—Synthesized from 3-(2-bromoacetyl)phenol⁴⁶ and formamide according to the general procedure to afford **4** as brown solid in 53% yield. mp=209–210 °C. TLC R_f =0.45 (20% MeOH:CHCl₃). ¹H NMR (CDCl₃ + CD₃OD) δ 7.69 (s, 1H), 7.33 (s, 1H), 7.22–7.17 (m, 3H), 6.75–6.68 (m, 1H). ¹³C NMR (CDCl₃ + CD₃OD) δ_d 158.7, 139.2, 135.4; δ_u 136.8, 130.8, 117.4, 117.0, 115.0, 112.8. IR (KBr) 3294, 2802, 1619, 1582, 1492, 1471 cm^{-1} . NP-HPLC t_R =10.81 (40:60, 2-propanol:n-hexane, 1 mL/min). MS m/z 160.

4-(3-Fluorophenyl)-1H-imidazole (5)—Synthesized from 2-bromo-(3-fluorophenyl)ethanone⁴⁸ and formamide according to the general procedure to afford **5** as off-white solid in 52% yield. mp=94–95 °C. TLC R_f =0.27 (10% MeOH:CHCl₃). ¹H NMR (CDCl₃) δ 10.06 (br s, 1H), 7.68 (d, 1H, J =0.72 Hz), 7.51 (d, 1H, J =11.76 Hz), 7.46–7.23 (m, 3H), 6.97–6.87 (m, 1H). ¹³C NMR (CDCl₃) δ_d 163.48 (J^1_{C-F} =243.34 Hz), 138.9, 135.7 (J^3_{C-F} =8.28 Hz); δ_u 135.9, 130.5 (J^3_{C-F} =8.52 Hz), 120.7 (J^4_{C-F} =2.74 Hz), 115.1, 113.9 (J^2_{C-F} =21.19 Hz), 112.05 (J^2_{C-F} =22.57 Hz). IR (KBr) 3057, 3000, 2861, 1607, 1561, 1511 cm^{-1} . NP-HPLC t_R =6.41 (30:70, 2-propanol:n-hexane, 1 mL/min). MS m/z 162.

3-(1H-imidazol-4-yl)benzotrile (6)—Synthesized from 3-(2-bromoacetyl)benzotrile⁵⁰ and formamide according to the general procedure to afford **6** as white solid in 43% yield. mp=191–192 °C. TLC R_f =0.63 (20% MeOH:CHCl₃). ¹H NMR (CDCl₃) δ 7.98–7.94 (m, 2H), 7.66 (d, 1H, J =1.05 Hz), 7.52–7.44 (m, 2H), 7.36 (d, 1H, J =1.08 Hz). NP-HPLC t_R =8.39 min 30:70 (2-propanol:n-hexane, 1 mL/min). MS m/z 169.

3-(1H-imidazol-4-yl)pyridine (7)—Synthesized from 2-bromo-1-(pyridine-3-yl)ethanone hydrobromide⁵¹ and formamide according to the literature procedure⁵² to afford **7** as yellow oil in 67% yield. TLC R_f =0.37 (20% MeOH:CHCl₃). ¹H NMR (CDCl₃) δ 9.01 (d, 1H, J =1.68 Hz), 8.48 (dd, 1H, J =1.59, 3.24 Hz), 8.09 (dt, 1H, J =1.83, 4.11 Hz), 7.78 (d, 1H, J =0.96 Hz), 7.45 (d, 1H, J =0.96 Hz), 7.36–7.32 (m, 1H). NP-HPLC t_R =30.19 (30:70, 2-propanol:n-hexane, 1 mL/min). MS m/z 145.

4-(1H-imidazol-4-yl)phenol (8)—Synthesized from 4-(2-bromoacetyl)phenol⁴⁶ and formamide following the general procedure to afford **8** as brown solid in 52% yield. mp=221–222 °C; lit 225–226 °C⁵³. TLC R_f =0.28 (20% MeOH:CHCl₃). ¹H NMR (CDCl₃ + CD₃OD) δ 7.66 (d, 1H, J =1.08 Hz), 7.53 (t, 1H, J =2.79 Hz), 7.50 (t, 1H, J =2.76 Hz), 7.23 (d, 1H, J =1.08 Hz), 6.83 (t, 1H, J =2.76 Hz), 6.80 (t, 1H, J =2.76 Hz). ¹³C NMR (CDCl₃ + CD₃OD) δ_d 157.9, 139.3, 125.9; δ_u 136.6, 127.4, 116.7, 116.1. IR (KBr) 3196, 2589, 1610, 1515 cm^{-1} . NP-HPLC t_R =11.53 (40:60, 2-propanol:n-hexane, 1 mL/min). MS m/z 160.

4-(4-Fluorophenyl)-1H-imidazole (9)—Synthesized from 2-bromo-(4-fluorophenyl)ethanone⁴⁸ and formamide according to the general procedure to afford **9** as off-white solid in 51% yield. mp=125–126 °C. TLC R_f =0.24 (10% MeOH:CHCl₃). ¹H NMR (CDCl₃) δ 10.67 (s, 1H), 7.70–7.74 (m, 3H), 7.26 (s, 1H), 7.08–7.00 (m, 2H). ¹³C NMR (CDCl₃) δ_d 162.2 (J^1_{C-F} =244.33 Hz), 138.6, 129.6; δ_u 135.9, 126.8 (J^3_{C-F} =7.94 Hz), 115.84 (J^2_{C-F} =21.48 Hz), 114.9. IR (KBr) 3099, 3053, 2858, 1658, 1606, 1562, 1465 cm⁻¹. NP-HPLC t_R =6.91 (30:70, 2-propanol:n-hexanes, 1mL/min). MS m/z 162.

4-(2,6-Dimethoxyphenyl)-1H-imidazole (10)—Synthesized from 2-bromo-1-(2,6-dimethoxyphenyl)ethanone⁵⁴ and formamide according to the general procedure to afford **10** as yellow oil in 65% yield. TLC R_f =0.43 (20% MeOH:CHCl₃). ¹H NMR (CDCl₃) δ 10.80 (br s, 1H), 7.70 (s, 1H), 7.63 (s, 1H), 7.13 (t, 1H, J =8.43 Hz), 6.61 (s, 1H), 6.58 (s, 1H), 3.82 (s, 6H). ¹³C NMR (CDCl₃) δ_d 156.6, 124.2, 107.8; δ_u 133.8, 129.3, 127.5, 124.4, 104.2, 103.8, 55.6 (2C). IR (film) 3417, 3118, 1589, 1483 cm⁻¹. NP-HPLC t_R =9.81 (30:70, 2-propanol:n-hexane, 1mL/min). MS m/z 204.

2-(1H-Imidazol-4-yl)benzene-1,3-diol (11)—The dimethoxy compound **10** (100 mg, 0.489 mmol) was heated to reflux (145–150 °C) in HBr (5 mL, 48% aq. solution) for 10 h. After cooling, excess of HBr was distilled off, the residue was diluted with MeOH (15 mL), treated with solid NaHCO₃ and filtered. The filtrate was taken in EtOAc (50 mL), washed with water, dried (Na₂SO₄) and concentrated *in vacuo* to afford light brown solid, which was purified by chromatography to afford **11** as off-white solid in 78% yield. mp=205–206 °C. TLC R_f =0.61 (20% MeOH:CHCl₃). ¹H NMR (CD₃OD) δ 7.73 (d, 1H, J =2.19 Hz), 6.89 (t, 1H, J =8.13 Hz), 6.40 (s, 1H), 6.37 (s, 1H). ¹³C NMR (CD₃OD) δ_d 157.6, 137.6, 107.2; δ_u 132.9, 128.3, 117.2, 108.0. IR (KBr) 3416, 3261, 1614, 1596 cm⁻¹. NP-HPLC t_R =11.60 (60:40, 2-propanol:n-hexane 0.5mL/min).

3-(1H-Imidazol-4-yl)benzaldehyde (12)—The nitrile was reduced with Raney Ni following a literature procedure.¹⁹ Chromatographic purification gave **12** as white solid in 71% yield. mp.137–138 °C. TLC R_f =0.57 (20% MeOH:CHCl₃). ¹H NMR (CDCl₃ + CD₃OD) δ 10.03 (s, 1H), 8.22 (t, 1H, J =1.50 Hz), 8.01 (dt, 1H, J =1.59, 4.89 Hz), 7.77 (dt, 1H, J =1.23, 5.04 Hz), 7.57 (t, 1H, J =7.68 Hz), 7.45 (s, 1H). NP-HPLC t_R =6.48 (40:60, 2-propanol:n-hexane, 0.5 mL/min).

General Procedure for the Suzuki coupling—A mixture of 4-bromo-imidazole (0.680 mmol), substituted thiomethylphenylboronic acid (0.748 mmol), Pd(OAc)₂ (0.0340 mmol), PPh₃ (0.102 mmol) and K₂CO₃ in n-propanol (7 mL) and water (2 mL) was heated to reflux for 24 h. After cooling, the reaction mixture was diluted with water (10 mL) and extracted with EtOAc (3 × 50 mL). The combined organic extract was dried (Na₂SO₄) and concentrated *in vacuo* to afford yellowish oil. Chromatographic purification afforded the desired products as white solid.

4-(2-(Methylthio)phenyl)-1H-imidazole (13)—Synthesized from 4-bromo-imidazole and 2-thiomethyl phenylboronic acid according to the general procedure to afford **13** as white crystalline solid in 31% yield. mp 123–125 °C. TLC R_f =0.52 (20% MeOH:CHCl₃). ¹H NMR (CDCl₃) δ 8.94 (br s, 1H), 7.70 (d, 1H, J =0.96 Hz), 7.66–7.63 (dd, 1H, J =1.62, 5.67 Hz), 7.46 (d, 1H, J =1.02 Hz), 7.32–7.17 (m, 3H), 2.42 (s, 3H). ¹³C NMR (CDCl₃) δ_d 135.6, 135.0, 131.6; δ_u 135.1, 129.4, 127.9, 127.5, 125.8, 121.1, 16.7. IR (KBr) 3060, 2872, 1586, 1463 cm⁻¹. NP-HPLC t_R =9.26 (20:80, 2-propanol:n-hexane, 1mL/min). MS m/z 190.

4-(3-(methylthio)phenyl)-1H-imidazole (14)—Synthesized from 4-bromo-imidazole and 3-thiomethyl phenylboronic acid according to the general procedure to afford **14** as

white crystalline solid in 57% yield. mp=126–127 °C. TLC R_f =0.50 (20% MeOH:CHCl₃). ¹H NMR (CDCl₃) δ 9.43 (br s, 1H), 7.70 (s, 1H), 7.65 (t, 1H, J =1.65 Hz), 7.48–7.45 (dt, J =1.32, 5.1 Hz), 7.35 (s, 1H), 7.27 (t, 1H, J =7.74 Hz), 7.15–7.12 (m, 1H). ¹³C NMR (CDCl₃) δ_d 139.3, 138.8, 133.9; δ_u 135.9, 129.4, 125.3, 123.2, 122.0, 115.7, 15.9. IR (KBr) 3109, 3052, 2810, 2620 cm⁻¹. NP-HPLC t_R =9.58 (20:80, 2-propanol:n-hexane, 1mL/min). MS m/z 190.

4-(4-(methylthio)phenyl)-1H-imidazole (15)—Synthesized from 4-bromo-imidazole and 4-thiomethyl phenyl boronic acid according to the general procedure to afford **15** as white crystalline solid in 37% yield. mp=155–156 °C. TLC R_f =0.51 (20% MeOH:CHCl₃). ¹H NMR (CDCl₃ + CD₃OD) δ 7.60 (m, 3H), 7.25 (m, 3H), 2.47 (s, 3H). ¹³C NMR (CDCl₃) δ_d 137.8, 136.8, 129.9; δ_u 135.7, 127.1, 125.3, 115.5. IR (KBr): 3055, 2810, 1544, 1494 cm⁻¹. NP-HPLC t_R =10.74 (20:80, 2-propanol:n-hexane, 1mL/min). MS m/z 190.

General Procedure for demethylation of Suzuki products^{20, 21}—To a solution of thiomethyl derivatives (0.263 mmole) in liq. NH (20 mL) at -78 °C was added Na metal until the blue color persisted for at least 15 min. Solid NH₄Cl (55 mg) was added, the solution was allowed to warm to rt., and NH₃ was evaporated with a stream of N₂. The solid residue was acidified by adding 6N HCl. The acidic solution was basified by adding NH₄OH solution and the precipitate so formed was filtered, washed with water and concentrated *in vacuo* to afford a white solid. Chromatographic purification afforded the final product as white solid.

2-(1H-imidazol-4-yl)benzenethiol (16)—Compound **16** was synthesized from **13** according to the general procedure for demethylation in 74% yield. mp=192–194 °C. TLC R_f =0.30 (20% MeOH:CHCl₃). ¹H NMR (CD₃OD) δ 7.89 (s, 1H), 7.60 (dd, 1H, J =5.92, 1.32 Hz), 7.49 (dd, 1H, J =5.55, 1.89 Hz), 7.38 (s, 1H), 7.28–7.19 (m, 2H). ¹³C NMR (CD₃OD) δ_d 136.7, 136.0, 133.7; δ_u 131.0, 129.6, 129.5, 128.4, 120.0. IR (KBr): 3400, 3090, 2842, 1638, 1457 cm⁻¹. NP-HPLC t_R =22.41 (40:60, 2-propanol:n-hexane, 0.5 mL/min).

3-(1H-imidazol-4-yl)benzenethiol (17)—Compound **17** was synthesized from **14** following the general procedure for demethylation in 80% yield. TLC R_f =0.30 (20% MeOH:CHCl₃). ¹H NMR (CDCl₃ + CD₃OD) δ 7.85 (t, 1H, J =1.53 Hz), 7.69 (s, 1H), 7.64 (s, 1H), 7.60–7.56 (dt, 1H, J =4.92, 1.23 Hz), 7.43–7.40 (dt, 1H, J =4.92, 1.23 Hz), 7.36–7.30 (m, 2H). ¹³C NMR (CDCl₃ + CD₃OD) δ_d 137.5 (2C), 133.8; δ_u 135.8, 129.3, 126.0, 124.0, 123.8, 115.7. IR (KBr) 3402, 3118, 3080, 1597 cm⁻¹. NP-HPLC t_R =27.90 (30:70, 2-propanol:n-hexane, 1 mL/min).

3-(4H-imidazol-4-yl)benzenethiol (18)—Compound **18** was synthesized from **15** following the general procedure for demethylation in 72% yield. mp=231–232 °C. TLC R_f =0.26 (20% MeOH:CHCl₃). ¹H NMR (CD₃OD) δ 7.83 (d, 1H J =1.08 Hz), 7.68 (t, 1H, J =2.16 Hz), 7.65 (t, 1H, J =2.01 Hz), 7.52 (t, 1H, J =2.07 Hz), 7.49 (t, 1H, J =1.92 Hz), 7.47 (d, 1H, J =1.08 Hz). ¹³C NMR (CD₃OD) δ_d 138.9, 136.8, 133.7; δ_u 137.3, 130.1, 126.8, 116.9. IR (KBr) 3399, 3084, 2848, 1457 cm⁻¹. NP-HPLC t_R =10.17 (40:40:20, 2-propanol:EtOAc:n-hexane; 1 mL/min).

1-Methyl-4-phenylimidazole (19)—To a suspension of NaH (83.2 mg, 3.47 mmol) in THF (20 mL) at 0 °C was added a solution of 4-phenylimidazole (500 mg, 3.47 mmol) in THF (5 mL) over a period of 5 min. After stirring the reaction mixture for 30 min., MeI (541.5 mg, 3.81 mmol) was added dropwise and the reaction was stirred for 3h. The reaction was quenched by adding satd. NH₄Cl solution. The product was extracted with EtOAc

(2×50 mL). The combined organic extract was dried (Na₂SO₄) and concentrated *in vacuo* to afford a yellow oil. Chromatographic purification (50% EtOAc:Hexanes) afforded **19** as an off-white crystalline solid in 13% yield; 34% of the unreacted 4-phenylimidazole was also recovered. mp=108–109 °C (lit.⁵⁵ mp=109–110 °C).⁵⁵ TLC R_f =0.18 (EtOAc). ¹H NMR (CDCl₃) δ 7.77 (s, 1H), 7.74 (s, 1H), 7.46 (s, 1H), 7.39–7.16 (m, 4H), 3.71 (s, 3H).

1-Benzyl-4-phenylimidazole (20)—compound **20** was prepared by an analogous procedure to **19**, but with benzyl bromide as the alkylating agent. The reaction afforded an off-white solid in 37% yield. mp 100–101 °C (lit.⁵⁶ mp 102–103 °C. TLC R_f =0.47 (EtOAc). ¹H NMR (CDCl₃) δ 7.77 (d, 1H, J =1.38 Hz), 7.74 (s, 1H), 7.57 (d, 1H, J =1.05 Hz), 7.39–7.17 (m, 9H), 5.11 (s, 2H).

2-(2-(4-Phenyl-1H-imidazol-1-yl)ethyl)isoindoline-1,3-dione (21)—To a suspension of NaH (83.2 mg, 3.47 mmol) in THF (20 mL) at 0 °C was added a solution of 4-phenylimidazole (500 mg, 3.47 mmol) in THF (5 mL) over a period of 5 min. After stirring the reaction mixture for 30 min., *N*-(2-bromoethyl)-phthalimide (3.81 mmol) was added as a solution in THF (5 mL) and the reaction was stirred overnight. The reaction was quenched by adding satd. NH₄Cl solution. The product was extracted with EtOAc (2×50 mL). The combined organic extract was dried (Na₂SO₄) and concentrated *in vacuo* to afford a yellow oil. Chromatographic purification (50% EtOAc:hexanes) afforded **21** as white crystalline solid in 38% yield. mp=150–151 °C. TLC R_f =0.23 (20% MeOH:CHCl₃). ¹H NMR (CDCl₃) δ 7.82–7.67 (m, 6H), 7.44 (s, 1H), 7.35–7.17 (m, 4H), 4.28 (t, 2H, J =6.65 Hz), 4.07 (t, 2H, J =6.60 Hz). ¹³C NMR (CDCl₃) δ_d 167.8, 142.9, 134.1, 131.1, 44.7, 38.3; δ_u 137.6, 134.4, 128.6, 126.9, 124.9, 123.7, 114.8.

2-(3-(4-Phenyl-1H-imidazol-1-yl)propyl)isoindoline-1,3-dione (22)—Compound **22** was prepared from *N*-(2-bromopropyl)phthalimide and 4-phenylimidazole according to the procedure for **21**. The product was obtained as white solid in 57% yield. mp=125–126 °C. TLC R_f =0.23 (20% MeOH:CHCl₃). ¹H NMR (CDCl₃) δ 7.85–7.68 (m, 6H), 7.57 (s, 1H), 7.37–7.19 (m, 4H), 4.03 (t, 1H, J =6.90 Hz), 3.79 (t, 1H, J =6.39 Hz), 2.24 (m, 2H). ¹³C NMR (CDCl₃) δ_d 168.1, 142.1, 134.1, 131.6, 44.6, 35.1, 29.8; δ_u 137.4, 133.9, 128.4, 126.5, 124.6, 123.1, 114.6.

2-(4-Phenyl-1H-imidazol-1-yl)ethanamine (23)—To a solution of **21** (100 mg, 0.315 mmol) in ethanol (5 mL) was added hydrazine hydrate (1mL) and the solution was stirred at 60 °C for 5 h. After cooling, the volatiles were evaporated; the crude product was diluted with ethylacetate (25 mL) and washed with water. The organic layer was dried (Na₂SO₄) and concentrated *in vacuo* to afford a yellow oil. Chromatographic purification afforded **23** as yellow oil in 51% yield. TLC R_f =0.23 (40% MeOH:CHCl₃). ¹H NMR (CDCl₃) δ 7.78–7.75 (m, 2H), 7.55 (d, 1H, J =0.99 Hz), 7.39–7.20 (m, 4H), 4.00 (t, 2H, J =5.85 Hz), 3.08 (t, 2H, J =5.79 Hz). ¹³C NMR (CDCl₃) δ_d 142.7, 134.3, 50.61, 42.8; δ_u 137.8, 128.8, 127.0, 124.9, 114.9. IR (film) 3431, 3251, 2940, 1652 cm⁻¹. RP-HPLC t_R =2.14 [20:80; H₂O:CH₃CN (0.1% TFA)]. MS m/z 187.

3-(4-Phenyl-1H-imidazol-1-yl)propan-1-amine (24)—Compound **24** was prepared by an analogous procedure to **23** affording a pale yellow oil in 67% yield. TLC R_f =0.20 (40% MeOH:CHCl₃). ¹H NMR (CDCl₃) δ 7.78–7.75 (m, 2H), 7.48 (d, 1H, J =1.11 Hz), 7.38–7.18 (m, 4H), 4.01 (t, 2H, J =6.96 Hz), 2.70 (t, 2H, J =6.75 Hz), 1.89 (m, 2H), 1.20 (br s, 2H). ¹³C NMR (CDCl₃) δ_d 142.3, 134.4, 44.4, 38.8, 29.7; δ_u 137.5, 128.7, 126.7, 124.8, 114.8. IR (CHCl₃) 3156, 3021, 2361, 1650 cm⁻¹. RP-HPLC t_R =2.13 [20:80; H₂O:CH₃CN (0.1% TFA)].

3-(4-Phenyl-1H-imidazol-1-yl)propanenitrile (25)—A mixture of 4-phenylimidazole (1.0 g, 6.93 mmol) and acrylonitrile (10 mL) was heated (140 °C) in a sealed tube for 24 h. After cooling the excess of acrylonitrile was removed under reduced pressure. Chromatographic purification of the crude gave **25** as off-white solid (1.03 g) in 75% yield. mp=110–112 °C (lit.⁵⁷ mp=112–113 °C). TLC R_f =0.34 (10% MeOH:CHCl₃). ¹H NMR (CDCl₃) δ 7.76 (s, 1H), 7.74 (s, 1H), 7.67–7.19 (m, 5H), 4.26 (t, 2H, J =6.45 Hz), 2.83 (t, 2H, J =6.42 Hz).

3-Benzyl-1-(2-cyanoethyl)-4-phenyl-1H-imidazol-3-ium bromide (26)—A mixture of **25** (500 mg, 2.53 mmol) and benzyl bromide (5.06 mmol) was heated to reflux in acetonitrile (20 mL) for 8 h. After cooling, the solvent was evaporated, the residue was diluted with diethyl ether, and filtered to afford an off-white solid (467 mg) in 96% yield. mp=151–153 °C. ¹H NMR (CDCl₃) δ 10.51 (s, 1H), 7.89 (s, 1H), 7.53–7.25 (m, 10H), 7.08–7.05 (m, 2H), 5.39 (s, 2H), 4.94 (t, 2H, J =6.21 Hz), 3.41 (t, 2H, J =6.21 Hz).

1-Benzyl-5-phenyl-1H-imidazole (27)—A solution of **26** (250 mg, 0.678 mmol) in MeOH (5 mL) was treated with NaOH (1.36 mmol in 5 mL H₂O). After 1 h, the reaction was acidified by adding 6N HCl and washed with diethyl ether. The acidic solution was adjusted to pH 9.0 by 25% aqueous NH₃ solution and extracted with EtOAc (3 × 35 mL). The organic extract was dried (Na₂SO₄) and concentrated *in vacuo* to afford **27** as an off-white crystalline solid (124 mg) in 78% yield. mp=114–115 °C (lit.²³ mp 112–113 °C). TLC R_f =0.64 (5% MeOH:CHCl₃). ¹H NMR (CDCl₃) δ 7.57 (s, 1H), 7.39–7.27 (m, 8H), 7.15 (s, 1H), 7.03–7.00 (m, 2H), 5.15 (s, 2H).

4-Phenyl-1-trityl-1H-imidazole-2-carbaldehyde (28)—To an ice cold (0 °C) solution of *N*-trityl-4-phenylimidazole²⁴ (0.500 g, 1.29 mmol) in THF (20 mL) was added *n*BuLi (0.889 mL of 1.6 M solution in hexanes, 1.41 mmol), the solution was warmed to rt and stirred for 2 h. After cooling to –78 °C, DMF (1 mL) was added, the reaction was allowed to warm to rt and stirring was continued for 3 h. The reaction mixture was diluted with water (10 mL) and extracted with CH₂Cl₂ (3 × 50 mL). The combined organic layer was washed with water, brine, dried (MgSO₄), and concentrated *in vacuo* to afford a yellowish oil. Chromatographic purification (10% EtOAc:hexanes) afforded **28** as white solid in 72% yield. mp=178–179 °C (lit.²⁴ mp=184 °C). TLC R_f =0.8 (25% EtOAc:hexanes). ¹H NMR (CDCl₃) 9.22 (s, 1H), 7.76 (d, 1H, J =1.38 Hz), 7.74 (s, 1H), 7.38–7.24 (m, 13H), 7.19–7.14 (m, 6H).

(4-Phenyl-1H-imidazol-2-yl)methanol (29)—To a solution of compound **28** (0.250g, 0.603 mmol) in methanol (10 mL) at 0 °C was added NaBH₄ (0.0684 g, 80 mmol) in three portions. After stirring for 2 h the solvent was removed *in vacuo*. The crude product was chromatographed to afford *N*-trityl **29** as a white solid in 92% yield. mp=195–196 °C (lit.²⁴ mp=195–196 °C). TLC R_f =0.23 (25% EtOAc:hexanes). ¹H NMR (CDCl₃ + CD₃OD) δ 7.70 (d, 1H, J =1.20 Hz), 7.67 (s, 1H), 7.35–7.31 (m, 11H), 7.21–7.15 (m, 8H), 3.66 (d, 2H, J =5.31 Hz), 3.37 (t, 1H, J =5.43 Hz).

The de-tritylation was achieved by refluxing *N*-trityl **29** (0.100 g, 0.240 mmol) in mixture of methanol (5 mL) and acetic acid (0.250 mL) for 4 h. After cooling, the volatiles were distilled-off and the crude was purified by chromatography to afford **29** as white crystalline solid in 90% yield. mp=197–198 °C (lit.²⁴ mp=199–200 °C). TLC R_f =0.22 (20% MeOH:CHCl₃). ¹H NMR (CD₃OD) δ 7.66 (m, 2H), 7.40–7.21 (m, 4H), 4.68 (s, 2H). NP-HPLC t_R =4.88 (40:60, 2-propanol:hexanes, 0.5mL/min). IR (KBr) 3154, 3037, 2768, 1604, 1534, 1457 cm⁻¹.

N-Methyl-1-(4-phenyl-1H-imidazol-2-yl)methanamine (30)—To a solution of **28** (0.500 g, 1.20 mmol) and *N*-methylamine hydrochloride (0.0896 g, 1.32 mmol) in CH₂Cl₂ (10 mL) was added triethylamine (0.133 g, 1.32 mmol) at 0 °C. After stirring for 5 h at 0 °C, NaBH₄ (3.6 mmol) was added followed by MeOH (2 mL), and reaction was warmed to rt and stirred for 2 h. The reaction mixture was acidified by careful addition of 6N HCl (3 mL) and heated to reflux for 2 h. After cooling to rt. The volatiles were evaporated and the crude was adjusted to pH 8–9 with 2N NaOH. The aqueous layer was extracted with CH₂Cl₂ (2 × 50 mL). The combined organic layer was dried (Na₂SO₄), and concentrated *in vacuo* to afford crude product. Chromatographic purification afforded **30** as a yellow glassy oil in 57% yield. TLC *R_f*=0.25 (20% MeOH:CHCl₃). ¹H NMR (CDCl₃) δ 7.67 (d, 1H, *J*=1.23 Hz), 7.65 (s, 1H), 7.34 (t, 2H, *J*=7.77 Hz), 7.24–7.19 (m, 2H), 5.39 (br s, 1H), 3.89 (s, 2H), 2.45 (s, 3H). ¹³C NMR (CDCl₃): δ_d 144.0, 138.2, 132.4, 47.1; δ_u 128.9, 127.3, 124.9, 34.4. IR (KBr): 3442, 3020, 2401, 1608, 1520 cm⁻¹. RP-HPLC *t_R*= 2.13 [20:80; H₂O:CH₃CN (0.1% TFA)].

5-Phenylthiazole (34)—Compound **34** was prepared according to the literature procedure⁴² in 73% yield as yellow solid. mp=42–43 °C (lit.⁵⁸ mp=44–45 °C). TLC *R_f*=0.40 (25% EtOAc:hexanes). ¹H NMR (CDCl₃) δ 8.75 (s, 1H), 8.08 (s, 1H), 7.60–7.56 (m, 2H), 7.44–7.31 (m, 3H). MS *m/z* 161.

3-Phenyl-1H-pyrazole (35)—Compound **35** was synthesized according to the literature procedure⁵⁹ in 35% yield as a white solid. mp=229–230 °C (lit.⁵⁹ mp=229–230 °C). TLC *R_f*=0.45 (5% MeOH:CHCl₃). ¹H NMR (CDCl₃): 7.87 (s, 1H), 7.53–7.50 (m, 2H), 7.40–7.35 (m, 2H), 7.24 (m, 1H).

3-(Furan-2-yl)pyridine (36)—Compound **36** was synthesized according to the literature procedure⁴⁴ in 65% yield as a yellowish oil. TLC *R_f*=0.26 (25% EtOAc:hexanes). ¹H NMR (CDCl₃) δ 8.93 (dd, 1H, *J*=1.62, 0.54 Hz), 8.48 (dd, 1H, *J*=3.27, 1.56 Hz), 7.92 (dt, 1H, *J*=4.11, 1.74 Hz), 7.52 (dd, 1H, *J*=1.17, 0.54 Hz), 7.32–7.26 (m, 1H), 6.74 (d, 1H, *J*=3.39 Hz), 6.50 (dd, 1H, *J*=1.80, 1.59 Hz). MS *m/z* 145.

Biochemical assays—Recombinant human IDO was expressed and purified as described.⁶⁰ The IC₅₀ inhibition assays were performed in a 96-well microtiter plate as described by Littlejohn et al.⁶⁰ with some modification. Briefly, the reaction mixture contained 50 mM potassium phosphate buffer (pH 6.5), 40 mM ascorbic acid, 400 μg/ml catalase, 20 μM methylene blue and ~27 nM purified recombinant IDO per reaction. The reaction mixture was added to the substrate, L-tryptophan (L-Trp), and the inhibitor. The inhibitors were serially diluted in 3-fold increments ranging from 100 μM to 1.69 nM and the L-Trp was tested at 100 μM (*K_m*=80 μM). The reaction was carried out at 37 °C for 60 min and stopped by the addition of 30% (w/v) trichloroacetic acid. The plate was incubated at 65 °C for 15 min to convert N-formylkynurenine to kynurenine and was then centrifuged at 1250 g for 10 min. Lastly, 100 μl supernatant from each well was transferred to a new 96 well plate and mixed at equal volume with 2% (w/v) p-dimethylamino-benzaldehyde in acetic acid. The yellow color generated from the reaction with kynurenine was measured at 490 nm using a Synergy HT microtiter plate reader (Bio-Tek, Winooski, VT). The data were analyzed using Graph Pad Prism 4 software (Graph Pad Software Inc., San Diego, CA). For the *K_i* determinations of **36**, **41**, and **50**, tryptophan concentrations were varied from 25–200 μM (*K_m*= 42 μM) and inhibitor concentrations were varied between 3-fold above and below the calculated IC₅₀. Otherwise, reaction conditions were exactly as described above. Data were analyzed with the Enzyme Kinetics module in SigmaPlot version 10.

Computational methods

Small molecule preparation—Molecules were constructed in MOE (MOE Molecular Operating Environment Chemical Computing Group, version 2005.06 Montreal Canada <http://www.chemcomp.com/>) ionized using MOE's WashMDB function and hydrogens were added. The small molecule conformation was minimized to a gradient of 0.01 in the MMFF94S force field^{61, 62} using distance-dependent dielectric constant of 1.

Protein preparation—Using the IDO crystal structure (PDB code 2D0T), hydrogen atoms were added and tautomeric states and orientations of Asn, Gln, His residues were determined with Molprobitry (<http://molprobitry.biochem.duke.edu/>).^{63, 64} Hydrogens were added to crystallographic waters using MOE.⁶⁵ The Amber99⁶⁶ force field in MOE was used and iron was parameterized in the Fe⁺³ state. Dioxygen was not added to the iron. All hydrogens were minimized to an rms gradient of 0.01 holding the remaining heavy atoms fixed. A stepwise minimization followed for all atoms using a quadratic force constant (100) to tether the atoms to their starting geometries; for each subsequent minimization, the force constant was reduced by a half until zero.

Docking calculations—The 2-[N-cyclohexylamino]ethane sulfonic acid and 4-phenyl-1-imidazole ligands were removed from the active site prior to docking. Preliminary docking calculations performed with annulin B were carried out using MolDock.⁶⁷ Gold (version 3.1)^{27, 28} and AutoDock (version 3.05)⁶⁸ were used with default parameters and reproduced the crystallographic position of 4-phenyl-1-imidazole binding to the heme. Docking of the naphthoquinone series of compounds using AutoDock and Gold produced a top scoring binding pose with a ketone oxygen within coordination distance to the heme iron.

Quantum Mechanical Calculations—Preliminary energy minimizations of all compounds in Table 1 and 2 were carried out using Molecular Operating Environment (MOE)⁶⁵. The force field MMFF94S^{61, 62} was used with a dielectric of 2 and energy minimization was terminated when the rms gradient fell below the cutoff value of 0.001 Å. The energy minimized geometries of all compounds were then exported from MOE for use in the Gaussian 03⁶⁹ suite of programs. Geometry optimizations were carried out using the *ab initio* Hartree Fock method, the B3LYP hybrid functional and Pople's basis set 6-31G(d,p). CHelpG charges were computed.⁷⁰ A table of the CHelpG charges for *o*, *m*, *p* substituted 4-phenylimidazole compounds is included in the Supporting Information.

Supplementary Material

Refer to Web version on PubMed Central for supplementary material.

Acknowledgments

Financial support for this work was provided by the National Institutes of Health (NCI R01 CA109542). A.J.M. is also the recipient of grants from the DoD Breast Cancer Research Program (BC044350), the State of Pennsylvania Department of Health (CURE/Tobacco Settlement Award), the Lance Armstrong Foundation, and the Concern Foundation. G.C.P. is the recipient of NIH grants CA82222 and CA100123. Additional support for this project was provided by grants to G.C.P. from the Charlotte Geyer Foundation and the Lankenau Hospital Foundation.

Abbreviations

CHES	N-cyclohexyl-2-aminoethanesulfonic acid
IDO	indoleamine 2,3-dioxygenase
1-MT	1-methyl-tryptophan

4-PI 4-phenyl-imidazole**REFERENCES**

1. Dunn GP, Old LJ, Schreiber RD. The immunobiology of cancer immunosurveillance and immunoediting. *Immunity*. 2004; 21:137–148. [PubMed: 15308095]
2. Zou W. Immunosuppressive networks in the tumour environment and their therapeutic relevance. *Nat. Rev. Cancer*. 2005; 5:263–74. [PubMed: 15776005]
3. Muller AJ, Scherle PA. Targeting the mechanisms of tumoral immune tolerance with small-molecule inhibitors. *Nat. Rev. Cancer*. 2006; 6:613–625. [PubMed: 16862192]
4. Muller AJ, Prendergast GC. Marrying immunotherapy with chemotherapy: why say IDO? *Cancer Res*. 2005; 65:8065–8. [PubMed: 16166276]
5. Munn DH, Mellor AL. Indoleamine 2,3-dioxygenase and tumor-induced tolerance. *J. Clin. Invest*. 2007; 117:1147–54. [PubMed: 17476344]
6. Muller AJ, DuHadaway JB, Donover PS, Sutanto-Ward E, Prendergast GC. Inhibition of indoleamine 2,3-dioxygenase, an immunoregulatory target of the cancer suppression gene Bin1, potentiates cancer chemotherapy. *Nat. Med*. 2005; 11:312–9. [PubMed: 15711557]
7. Sono M, Roach MP, Coulter ED, Dawson JH. Heme-Containing Oxygenases. *Chem. Rev*. 1996; 96:2841–2888. [PubMed: 11848843]
8. Botting NP. Chemistry and Neurochemistry of the Kynurenine Pathway of Tryptophan Metabolism. *Chem. Soc. Rev*. 1995; 24:401–12.
9. Sono M, Hayaishi O. The Reaction Mechanism of Indoleamine 2,3-Dioxygenase. *Biochem. Reviews*. 1980; 50:173–81.
10. Cady SG, Sono M. 1-Methyl-DL-tryptophan, beta-(3-benzofuranyl)-DL-alanine (the oxygen analog of tryptophan), and beta-[3-benzo(b)thienyl]-DL-alanine (the sulfur analog of tryptophan) are competitive inhibitors for indoleamine 2,3-dioxygenase. *Arch. Biochem. Biophys*. 1991; 291:326–33. [PubMed: 1952947]
11. Peterson AC, Migawa MT, Martin MJ, Hamaker LK, Czerwinski KM, Zhang W, Arend RA, Fisette PL, Ozaki Y, Will JA, Brown RR, Cook JM. Evaluation of functionalized tryptophan derivatives and related compounds as competitive inhibitors of indoleamine 2,3-dioxygenase. *Med. Chem. Res*. 1994; 3:531–544.
12. Pereira A, Vottero E, Roberge M, Mauk AG, Andersen RJ. Indoleamine 2,3-dioxygenase inhibitors from the Northeastern Pacific Marine Hydroid *Garveia annulata*. *J. Nat. Prod*. 2006; 69:1496–9. [PubMed: 17067170]
13. Brastianos HC, Vottero E, Patrick BO, Van Soest R, Matainaho T, Mauk AG, Andersen RJ. Exiguamine A, an indoleamine-2,3-dioxygenase (IDO) inhibitor isolated from the marine sponge *Neopetrosia exigua*. *J. Am. Chem. Soc*. 2006; 128:16046–7. [PubMed: 17165752]
14. Carr G, Chung MKW, Mauk AG, Andersen RJ. Synthesis of Indoleamine 2,3-Dioxygenase Inhibitory Analogues of the Sponge Alkaloid Exiguamine A. *J. Med. Chem*. 2008; 51:2634–2637. [PubMed: 18393489]
15. Kumar S, Malachowski WP, DuHadaway JB, LaLonde JM, Carroll PJ, Jaller D, Metz R, Prendergast GC, Muller AJ. Indoleamine 2,3-Dioxygenase Is the Anticancer Target for a Novel Series of Potent Naphthoquinone-Based Inhibitors. *J. Med. Chem*. 2008; 51:1706–1718. [PubMed: 18318466]
16. Sono M, Cady SG. Enzyme kinetic and spectroscopic studies of inhibitor and effector interactions with indoleamine 2,3-dioxygenase. 1. Norharman and 4-phenylimidazole binding to the enzyme as inhibitors and heme ligands. *Biochem*. 1989; 28:5392–5399. [PubMed: 2789076]
17. Sugimoto H, Oda S, Otsuki T, Hino T, Yoshida T, Shiro Y. Crystal structure of human indoleamine 2,3-dioxygenase: catalytic mechanism of O₂ incorporation by a heme-containing dioxygenase. *Proc. Natl. Acad. Sci. U S A*. 2006; 103:2611–6. [PubMed: 16477023]
18. Overberger CG, Shen C-M. Intramolecular base-catalyzed imidazole catalysis. *J. Am. Chem. Soc*. 1971; 93:6992–6998.

19. Tanaka A, Terasawa T, Hagihara H, Sakuma Y, Ishibe N, Sawada M, Takasugi H, Tanaka H. Inhibitors of Acyl-CoA:Cholesterol O-Acyltransferase. 2. Identification and Structure-Activity Relationships of a Novel Series of N-Alkyl-N-(heteroaryl-substituted benzyl)-N'-arylureas. *J. Med. Chem.* 1998; 41:2390–2410. [PubMed: 9632372]
20. Adams R, Ferretti A. Thioethers from halogen compounds and cuprous mercaptides. III. Preparation of aromatic di- and trimercapto compounds by dealkylation of aryl alkyl thioethers. *J. Am. Chem. Soc.* 1959; 81:4939–40.
21. Goerdeler J, Kandler J. Oxidation studies on some aminomercaptans. *Chem. Ber.* 1959; 92:1679–94.
22. Wright WB, Press JB, Chan PS, Marsico JW, Haug MF, Lucas J, Tauber J, Tomcufcik AS. Thromboxane synthetase inhibitors and antihypertensive agents. 1. N-[(1H-imidazol-1-yl)alkyl]aryl amides and N-[(1H-1,2,4-triazol-1-yl)alkyl]aryl amides. *J. Med. Chem.* 1986; 29:523–530. [PubMed: 3959030]
23. Horvath A. Michael Adducts in the Regioselective Synthesis of N-Substituted Azoles. *Syn.* 1995:1183–1189.
24. Magdolen P, Vasella A. Monocyclic, substituted imidazoles as glycosidase inhibitors. *Helv. Chim. Acta.* 2005; 88:2454–2469.
25. Gaspari P, Banerjee T, Malachowski WP, Muller AJ, Prendergast GC, DuHadaway J, Bennett S, Donovan AM. Structure-activity study of brassinin derivatives as indoleamine 2,3-dioxygenase inhibitors. *J. Med. Chem.* 2006; 49:684–92. [PubMed: 16420054]
26. Sono and Cady (ref. 11) report a K_i of 4.4 μM , but this assay was conducted with the much weaker substrate D-Trp.
27. Verdonk ML, Cole JC, Hartshorn MJ, Murray CW, Taylor RD. Improved Protein-Ligand Docking Using GOLD. *Proteins.* 2003; 52:609–623. [PubMed: 12910460]
28. Jones G, Willet P, Glen RC, Leach AR, Taylor R. Development And Validation Of A Genetic Algorithm For Flexible Docking. *J. Mol. Biol.* 1997; 267:727–748. [PubMed: 9126849]
29. Conway ME, Yennawar N, Wallin R, Poole LB, Hutson SM. Identification of a Peroxide-Sensitive Redox Switch at the CXXC Motif in the Human Mitochondrial Branched Chain Aminotransferase. *Biochem.* 2002; 41:9070–9078. [PubMed: 12119021]
30. Yennawar NH, Conway ME, Yennawar HP, Farber GK, Hutson SM. Crystal Structures of Human Mitochondrial Branched Chain Aminotransferase Reaction Intermediates: Ketimine and Pyridoxamine Phosphate Forms. *Biochem.* 2002; 41:11592–11601. [PubMed: 12269802]
31. Wood ZA, Poole LB, Karplus PA. Structure of Intact AhpF Reveals a Mirrored Thioredoxin-like Active Site and Implies Large Domain Rotations during Catalysis. *Biochem.* 2001; 40:3900–3911. [PubMed: 11300769]
32. Letcher TM, Bricknell BC. Calorimetric Investigation of the Interactions of Some Hydrogen-Bonded Systems at 298.15 K. *J. Chem. Eng. Data.* 1996; 41:166–169.
33. Desiraju, GR.; Steiner, T. *The Weak Hydrogen Bond in Structural Chemistry and Biology.* Oxford University Press; New York: 1999. p. 258-263.
34. Karty JM, Wu Y, Brauman JI. The RS--HSR Hydrogen Bond: Acidities of alpha,omega-Dithiols and Electron Affinities of Their Monoradicals. *J. Am. Chem. Soc.* 2001; 123:9800–9805. [PubMed: 11583541]
35. Konno T, Haneishi K, Hirotsu M, Yamaguchi T, Ito T, Yoshimura T. The First Triple Thiol-thiolate Hydrogen Bond versus Triple Diselenide Bond That Bridges Two Metal Centers. *J. Am. Chem. Soc.* 2003; 125:9244–9245. [PubMed: 12889924]
36. Müller K, Faeh C, Diederich F. Fluorine in pharmaceuticals: looking beyond intuition. *Science.* 2007; 317:1881–6. [PubMed: 17901324]
37. Otto HH, Schirmeister T. Cysteine Proteases and Their Inhibitors. *Chem. Rev.* 1997; 97:133–172. [PubMed: 11848867]
38. Margolin N, Raybuck SA, Wilson KP, Chen W, Fox T, Gu Y, Livingston DJ. Substrate and inhibitor specificity of interleukin-1 β -converting enzyme and related caspases. *J. Biol. Chem.* 1997; 272:7223–8. [PubMed: 9054418]

39. Garcia-Calvo M, Peterson EP, Leiting B, Ruel R, Nicholson DW, Thornberry NA. Inhibition of human caspases by peptide-based and macromolecular inhibitors. *J. Biol. Chem.* 1998; 273:32608–32613. [PubMed: 9829999]
40. Privett HK, Reedy CJ, Kennedy ML, Gibney BR. Nonnatural Amino Acid Ligands in Heme Protein Design. *J. Am. Chem. Soc.* 2002; 124:6828–6829. [PubMed: 12059195]
41. Vashi PR, Marques HM. The coordination of imidazole and substituted pyridines by the hemeoctapeptide N-acetyl-ferromicroperoxidase-8 (FeIINAcMP8). *J. Inorg. Biochem.* 2004; 98:1471–1482. [PubMed: 15337599]
42. Parisien M, Valette D, Fagnou K. Direct Arylation Reactions Catalyzed by Pd(OH)₂/C: Evidence for a Soluble Palladium Catalyst. *J. Org. Chem.* 2005; 70:7578–7584. [PubMed: 16149786]
43. Escribano FC, Derri Alcantara MP, Gomez-Sanchez A. Heterocycle formation from 1,3-dinitroalkanes. A novel pyrazole synthesis. *Tet. Lett.* 1988; 29:6001–6004.
44. Arcadi A, Burini A, Cacchi S, Delmastro M, Marinelli F, Pietroni B. The Palladium-Catalyzed Cross Coupling of Vinyl and Aryl Triflates with 2-Furylzinc Chloride: An Efficient Route to 2-Vinyl- and 2-Arylfurans. *Synlett.* 1990:47–48.
45. Eguchi N, Watanabe Y, Kawanishi K, Hashimoto Y, Hayaishi O. Inhibition of Indoleamine 2,3-Dioxygenase and Tryptophan 2,3-Dioxygenase by beta-Carboline and Indole Derivatives. *Arch. Biochem. Biophys.* 1984; 232:602–609. [PubMed: 6431906]
46. Black DS, Kumar N, McConnell DB. Synthesis of tethered indoles in the search for conformationally controlled calixindoles: an indole 3-substituent tether. *Tet.* 2001; 57:2203–2211.
47. Pandit UK, Bruice TC. Imidazole catalysis. VII. Dependence of imidazole catalysis of ester hydrolysis on the nature of the acyl group. *J. Am. Chem. Soc.* 1960; 82:3386–3390.
48. Henry RA, Hollins RA, Lowe-Ma C, Moore DW, Nissan RA. Anomalous reaction of pentafluorophenacyl bromide with hexamethylenetetramine. Structure of the product. *J. Org. Chem.* 1990; 55:1796–1801.
49. Perrone R, Berardi F, Leopoldo M, Tortorella V, Lograno MD, Daniele E, Govoni S. Oxygen isosteric derivatives of 3-(3-hydroxyphenyl)-N-n-propylpiperidine. *J. Med. Chem.* 1992; 35:3045–3049. [PubMed: 1354263]
50. Watson CY, Whish WJD, Threadgill MD. Synthesis of 3-substituted benzamides and 5-substituted isoquinolin-1(2H)-ones and preliminary evaluation as inhibitors of poly(ADP-ribose)polymerase (PARP). *Bio. Med. Chem.* 1998; 6:721–734.
51. Barlin GB, Davies LP, Ireland SJ, Ngu MML. Imidazo[1,2-b]pyridazines. VI. Syntheses and central nervous system activities of some 6-(alkoxy- and methylthio-phenoxy and methoxybenzylthio)-3-methoxy-2-phenyl(substituted phenyl and pyridinyl)imidazo[1,2-b]pyridazines. *Aust. J. Chem.* 1989; 42:1735–1748.
52. Kirchoff EW, Anderson DR, Zhang S, Cassidy CS, Flavin MT. Automated Process Research and the Optimization of the Synthesis of 4(5)-(3-Pyridyl)imidazole. *Org. Proc. Res. Dev.* 2001; 5:50–53.
53. Jones H, Fordice MW, Greenwald RB, Hannah J, Jacobs A, Ruyle WV, Walford GL, Shen TY. Synthesis and analgesic-antiinflammatory activity of some 4- and 5-substituted heteroarylsalicylic acids. *J. Med. Chem.* 1978; 21:1100–4. [PubMed: 309948]
54. Kiyama, R.; Kanda, Y.; Tada, Y.; Fujishita, T.; Kawasuji, T.; Takechi, S.; Fuji, M. Preparation of heterocyclic compounds as integrase inhibiting antiviral agents. 2003. WO2003016275
55. Pavlik JW, Kebede N. Photochemistry of Phenyl-Substituted 1-Methylpyrazoles. *J. Org. Chem.* 1997; 62:8325–8334. [PubMed: 11671969]
56. Nunami, K.-i.; Yamada, M.; Fukui, T.; Matsumoto, K. A Novel Synthesis of Methyl 1,5-Disubstituted Imidazole-4-carboxylates Using 3-Bromo-2-isocyanoacrylates (BICA). *J. Org. Chem.* 1994; 59:7635–7642.
57. Iradyan MA, Torosyan AG, Mirzoyan RG, Badalyants IP, Isaakyan ZS, Manucharyan DS, Dayan MK, Sakanyan GS, Dzhagatspanyan IA. Imidazole derivatives. XIII. Synthesis and pharmacological activity of some 1,4,5-substituted imidazoles. *Khim.-Farm. Zhurnal.* 1977; 11:42–48.

58. Pavlik JW, Tongcharoensirikul P, Bird NP, Day AC, Barltrop JA. Phototransposition Chemistry of Phenylisothiazoles and Phenylthiazoles. 1. Interconversions in Benzene Solution. *J. Am. Chem. Soc.* 1994; 116:2292–300.
59. Cabrera Escribano F, Derri Alcantara MP, Gomez-Sanchez A. Heterocycle formation from 1,3-dinitroalkanes. A novel pyrazole synthesis. *Tet. Lett.* 1988; 29:6001–4.
60. Littlejohn TK, Takikawa O, Skylas D, Jamie JF, Walker MJ, Truscott RJ. Expression and purification of recombinant human indoleamine 2, 3-dioxygenase. *Protein Expr. Purif.* 2000; 19:22–9. [PubMed: 10833386]
61. Halgren TA. MMFF VI. MMFF94s option for energy minimization studies. *J. Comput. Chem.* 1999; 20:720–729.
62. Halgren TA. MMFF VII. Characterization of MMFF94, MMFF94s, and other widely available force fields for conformational energies and for intermolecular-interaction energies and geometries. *J. Comput. Chem.* 1999; 20:740–774.
63. Word JM, Lovell SC, Richardson JS, Richardson DC. Asparagine and glutamine: Using hydrogen atom contacts in the choice of side-chain amide orientation. *J. Mol. Biol.* 1999; 285:1735–1747. [PubMed: 9917408]
64. Lovell SC, Davis IW, Arendall WB III, de Bakker PIW, Word JM, Prisant MG, Richardson JS, Richardson DC. Structure Validation by α Geometry: ϕ, ψ and $C\beta$ Deviation. *Proteins: Struct., Funct. and Genetics.* 2003; 50:437–450.
65. Inc., C. C. G.. MOE (Molecular Operating Environment). Montreal; Quebec, Canada: Jun. 2005 2005
66. Ponder JW, Case DA. Force Fields for Protein Simulations. *Adv. Prot. Chem.* 2003; 66:27–85.
67. Thomsen R, Christensen MH. MolDock: A New Technique for High-Accuracy Molecular Docking. *J. Med. Chem.* 2006; 49:3315–3321. [PubMed: 16722650]
68. Morris GM, Goodsell DS, Halliday RS, Huey R, Hart WE, Belew RK, Olson AJ. Automated Docking Using a Lamarckian Genetic Algorithm and and Empirical Binding Free Energy Function. *J. Comput. Chem.* 1998; 19:1639–1662.
69. Frisch, MJ.; Trucks, GW.; Schlegel, HB.; Scuseria, GE.; Robb, MA.; Cheeseman, JR.; Montgomery, JA., Jr.; Vreven, T.; Kudin, KN.; Burant, JC.; Millam, JM.; Iyengar, SS.; Tomasi, J.; Barone, V.; Mennucci, B.; Cossi, M.; Scalmani, G.; Rega, N.; Petersson, GA.; Nakatsuji, H.; Hada, M.; Ehara, M.; Toyota, K.; Fukuda, R.; Hasegawa, J.; Ishida, M.; Nakajima, T.; Honda, Y.; Kitao, O.; Nakai, H.; Klene, M.; Li, X.; Knox, JE.; Hratchian, HP.; Cross, JB.; Bakken, V.; Adamo, C.; Jaramillo, J.; Gomperts, R.; Stratmann, RE.; Yazyev, O.; Austin, AJ.; Cammi, R.; Pomelli, C.; Ochterski, JW.; Ayala, PY.; Morokuma, K.; Voth, GA.; Salvador, P.; Dannenberg, JJ.; Zakrzewski, VG.; Dapprich, S.; Daniels, AD.; Strain, MC.; Farkas, O.; Malick, DK.; Rabuck, AD.; Raghavachari, K.; Foresman, JB.; Ortiz, JV.; Cui, Q.; Baboul, AG.; Clifford, S.; Cioslowski, J.; Stefanov, BB.; Liu, G.; Liashenko, A.; Piskorz, P.; Komaromi, I.; Martin, RL.; Fox, DJ.; Keith, T.; Al-Laham, MA.; Peng, CY.; Nanayakkara, A.; Challacombe, M.; Gill, PMW.; Johnson, B.; Chen, W.; Wong, MW.; Gonzalez, C.; Pople, JA. Gaussian 03, Revision B.05. Gaussian, Inc.; Wallingford, CT: 2004. Revision B.05
70. Breneman CM, Wiberg KB. Determining atom-centered monopoles from molecular electrostatic potentials. The need for high sampling density in formamide conformational analysis. *J. Comput. Chem.* 1990; 11:361.

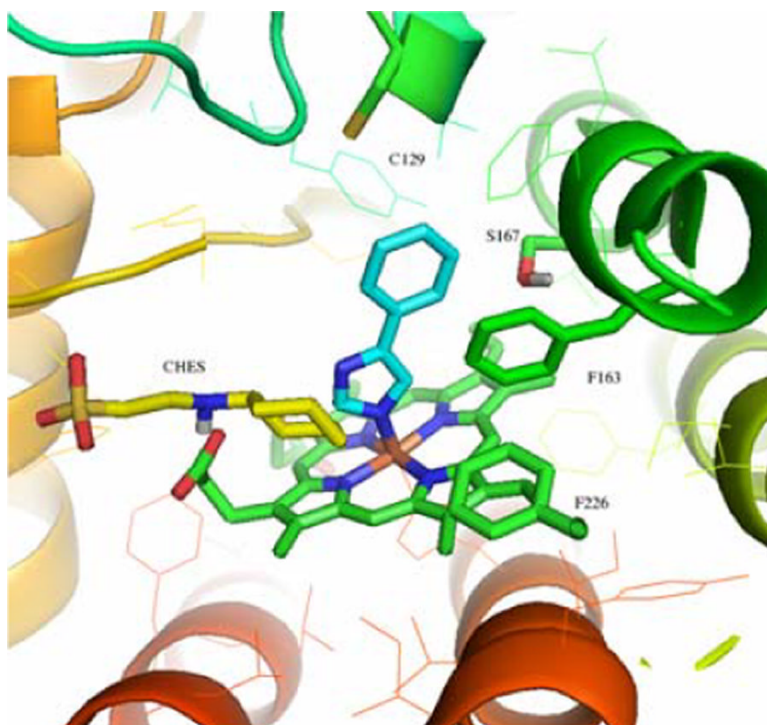


Figure 1. 4-PI bound to heme iron of IDO. C129 is located above the 4-PI phenyl ring, while S167 resides in the back of the binding site. The buffer molecule CHES (yellow) is bound at the entrance of the active site of the IDO crystal structure. Graphics generated with PyMOL 1.0, [<http://www.pymol.org>] an open-source molecular graphics system developed, supported and maintained by DeLano Scientific LLC. <http://www.delanoscientific.com>.

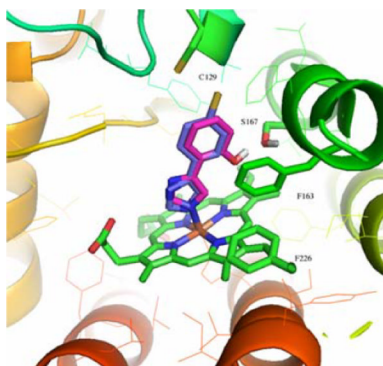


Figure 2. Predicted binding modes for 2-OH (**1**, magenta) and 4-SH (**18**, purple) as docked in Gold.^{27, 28} Figure rendered with PyMOL 098, (<http://www.pymol.org>), an open-source molecular graphics system developed, supported and maintained by DeLano Scientific LLC (<http://www.delanoscientific.com>).

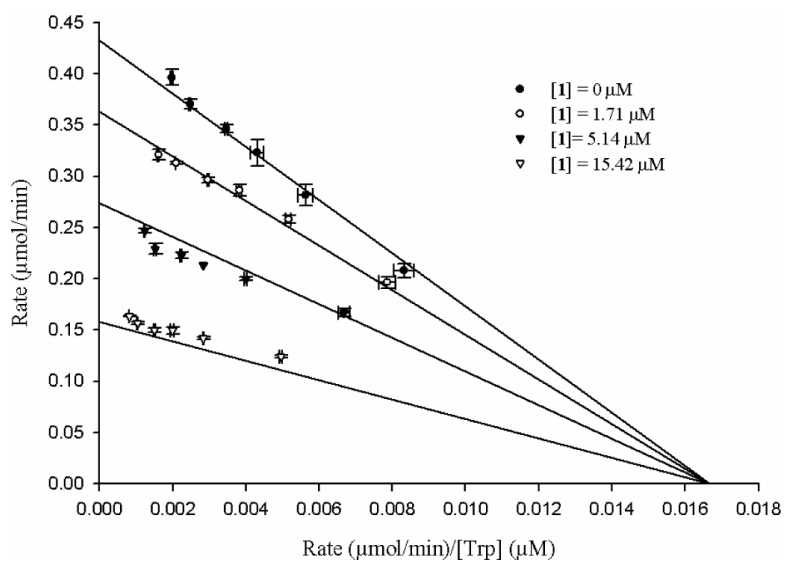
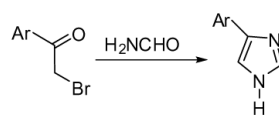


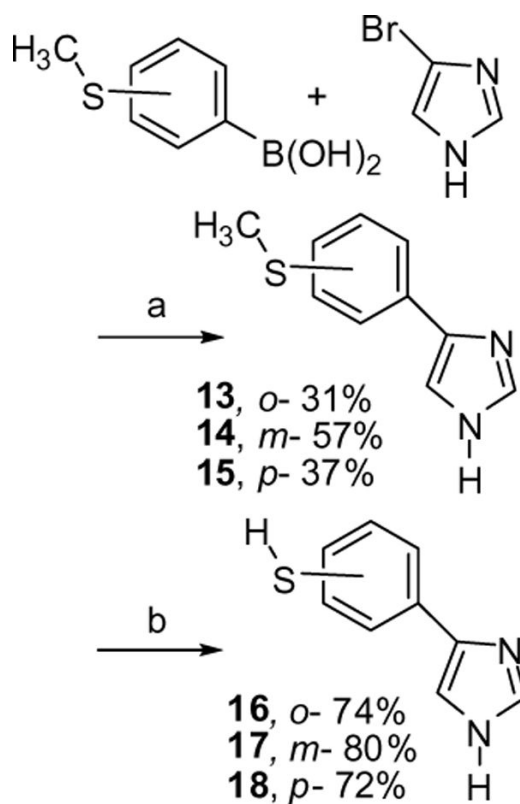
Figure 3.
Eadie-Hofstee plot for compound **1**.



Ar	Compound	% Yield
2-OH-Ph	1	49
2-F-Ph	2	52
thiophen-2-yl	3	60
3-OH-Ph	4	53
3-F-Ph	5	52
3-CN-Ph ¹⁹	6	43
3-pyridyl	7	67
4-OH-Ph	8	52
4-F-Ph	9	51
2,6-(OCH ₃) ₂ -Ph	10	65
2,6-(OH) ₂ -Ph	11	78

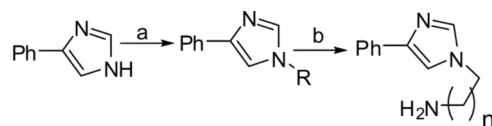
Scheme 1.

Derivatives synthesized by de novo imidazole synthesis.

**Scheme 2.**

Reagents and conditions: (a) Pd(OAc)₂, PPh₃, K₂CO₃, n-propanol:H₂O (7:3), reflux, 24h.

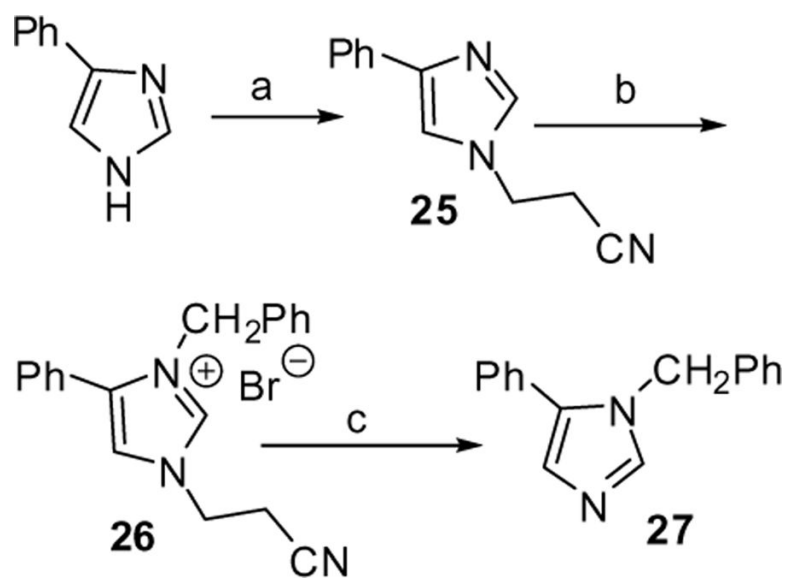
(b) Na, Liq. NH₃, NH₄Cl.



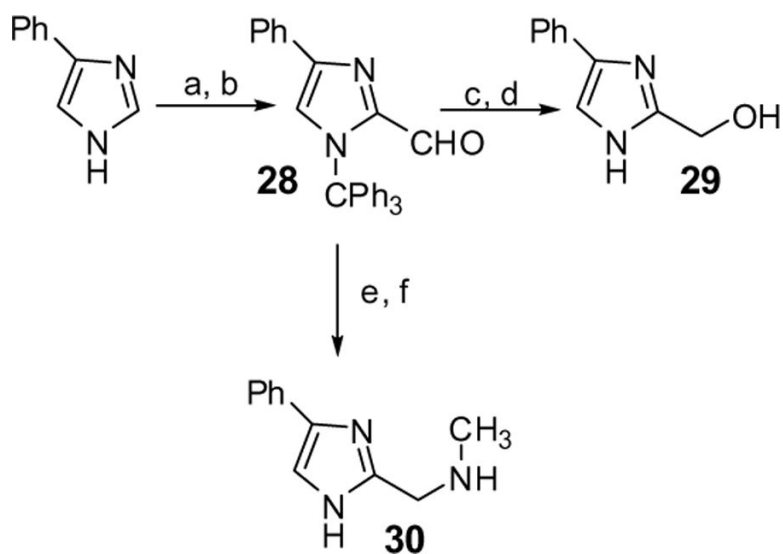
R	Compd.	a, % yd	Compd.	b, % yd
-CH ₃	19	13	-	-
-CH ₂ Ph	20	37	-	-
-	21	38	23	51
CH ₂ CH ₂ -			(n=1)	
N-				
phthaloyl				
-	22	57	24	67
CH ₂ CH ₂ C			(n=2) ²²	
H ₂ -N-				
phthaloyl				

Scheme 3.

Reagents and conditions: (a) NaH, THF, R-Br or CH₃-I, 0°C-rt, 3–12 h. (b) H₂NNH₂.xH₂O, EtOH, 65°C, 6h.

**Scheme 4.**

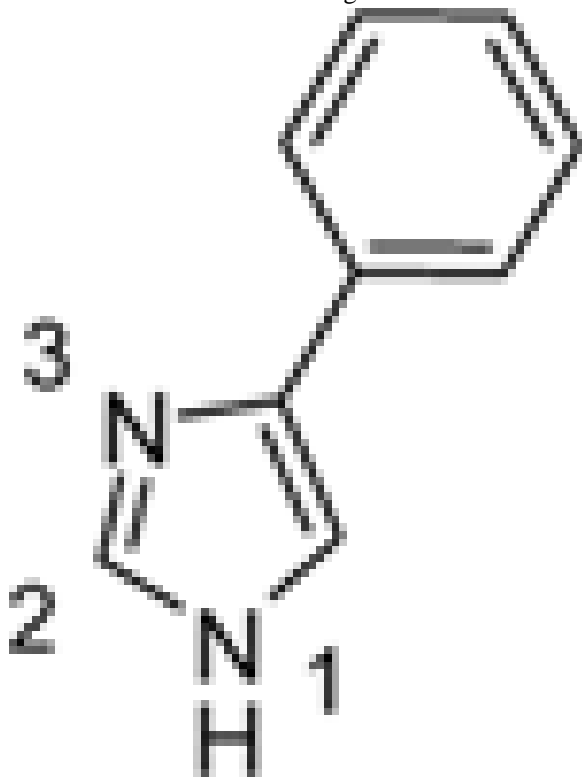
Reagents and conditions: (a) CH₂CHCN, sealed tube, 140°C, 1 d, 75% (b) PhCH₂Br, CH₃CN, reflux, 96%. (c) NaOH, MeOH, rt. 78%.

**Scheme 5.**

Reagents and conditions: (a) NEt_3 , Ph_3CCl , DMF, rt, 2h, 87% (b) nBuLi , DMF, 0°C -rt, 3h, 72% (c) NaBH_4 , MeOH, rt, 2h, 92% (d) AcOH , MeOH, 70°C , 4h, 90%. (e) $\text{H}_3\text{CNH}_2\cdot\text{HCl}$, NEt_3 , CH_2Cl_2 , MeOH, NaBH_4 , 0°C -rt, 7h. (f) MeOH, HCl, 70°C , 1h, 57% for two steps.

Table 1

IDO inhibition of imidazole ring substituted derivatives.

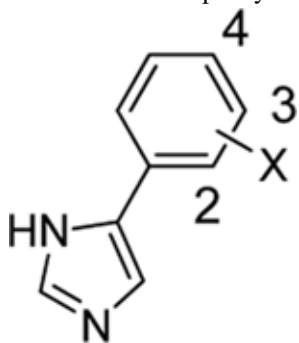


Compd	N-1	C-2	N-3	IC ₅₀ , μM ^a
27	—	H	PhCH ₂	32
4-PI	H	H	—	48 ²⁶
19	H ₃ C	H	—	N.I.
20	PhCH ₂	H	—	N.I.
23	H ₂ N(CH ₂) ₂	H	—	N.I.
24	H ₂ N(CH ₂) ₃	H	—	N.I.
29	H	HOCH ₂	—	N.I.
30	H	(H ₃ C)NHCH ₂	—	N.I.

^aValues are means of at least two experiments, standard deviation is given in parentheses (N.I.=no inhibition).

Table 2

IDO inhibition of phenyl ring substituted derivatives.

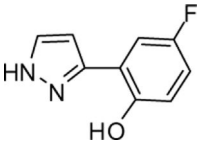
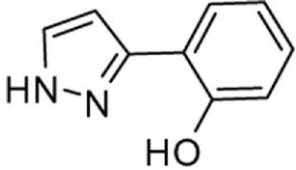
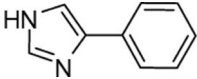
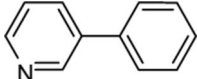
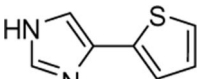
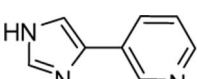
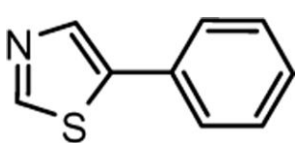
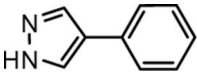
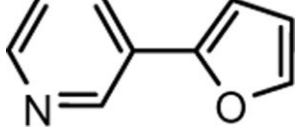


Compd.	X	IC ₅₀ , μM ^a
1	2-OH	4.8
11	2,6-(OH) ₂	5.3
17	3-SH	7.6
18	4-SH	7.7
16	2-SH	25
13	2-SCH ₃	38
7	3-CN	41
4-PI	H	48 ²⁶
5	3-F	60
14	3-SCH ₃	73
9	4-F	123
2	2-F	179
15	4-SCH ₃	209
4	3-OH	365
10	2,6-(OCH ₃) ₂	734
12	3-CHO	825
8	4-OH	1200

^aValues are means of at least two experiments, standard deviation is given in parentheses (N.I.=no inhibition).

Table 3

IDO inhibition of aromatic ring modified derivatives.

Compound	Structure	IC ₅₀ , μM ^a
31		26
32		35
4-PI		48 ²⁶
33		161
3		422
7		N.I.
34 ⁴²		N.I.
35 ⁴³		N.I.
36 ⁴⁴		N.I.

^a values are means of at least two experiments, standard deviation is given in parentheses (N.I.=no inhibition).

Table 4

Inhibition constants of three potent 4-PI derivatives

compound	$K_i(\mu\text{M})$
1	8.9
17	5.3
18	4.8